

RADIO SHOT: THROUGH-THE-WALL HUMAN RECOGNITION

Qinyi Xu^{*†} Yan Chen^{‡†} BeiBei Wang^{*†} K. J. Ray Liu^{*†}

^{*} University of Maryland, College Park, MD 20742 USA

[†] Origin Wireless, Inc., Greenbelt, MD 20770 USA

[‡] University of Electronic Science and Technology of China, Chengdu, China

Email: {qinyixu, bebewang, kjrlui}@umd.edu, eecyan@uestc.edu.cn

ABSTRACT

In this work, we show the existence of human radio biometrics and present a human identification system that can discriminate individuals even through the walls in a non-line-of-sight condition. Using commodity WiFi devices, the proposed system captures the channel state information (CSI) and extracts human radio biometric information from WiFi signals using time-reversal (TR) technique. By leveraging the fact that broadband wireless CSI has significant number of multipaths, which can be altered by human body interferences, the proposed system can recognize individuals in the TR domain without line-of-sight path. We built a prototype of the TR human identification system using standard WiFi chipsets with 3×3 MIMO transmission. The performance of the proposed system is evaluated and validated through multiple experiments. In general, the TR human identification system achieves an accuracy of 98.78% for identifying about a dozen of individuals using a single transmitter and receiver pair.

Index Terms— Human radio biometrics; time-reversal (TR); through-the-wall human identification; radio shot; broadband wireless.

1. INTRODUCTION

Nowadays, the capability of performing reliable human identification and recognition has become a crucial requirement in many applications, such as forensics, airport custom check, and bank securities. Biometric recognition refers to the automated recognition of individuals based on their human biological and behavioral characteristics [1]. The well-known biometrics for human recognition include fingerprint, face, iris, and voice. Since biometrics are inherent and distinctive to an individual, biometric traits are widely used in surveillance systems for human identification. All existing solutions require either special sensors to extract biometric traits, or a line-of-sight (LOS) path between the human and sensors, such as the photo shots and the retina scanning.

In contrast, in this paper, we focus on recognizing human individuals through the walls using WiFi signals with-

out carrying or deploying special sensors. Because human body acts as an interference in the indoor environment [2] and different body tissues have distinct reflectivities, permittivities and conductivities, WiFi signals will be affected differently when propagating to different individuals. The human-affected wireless signal with attenuation and alteration, which contains the unique identity information, is defined as *human radio biometrics*. To the best of our knowledge, this is the first effort to show and verify the existence of human radio biometrics, which can be found embedding in the wireless channel state information (CSI). Moreover, we propose a human recognition system that extracts the radio biometrics as features from the CSI for differentiating between people through the wall. The process for extracting human radio biometrics from WiFi signals is called *radio shot*.

To achieve this goal, we utilize the time-reversal (TR) technique to capture the differences between human radio biometrics and to reduce the dimension of features. TR technique takes advantage of the multipath propagation to produce a spatial-temporal resonance effect. A typical TR wireless communication system is shown in Figure 1 [3]. Suppose the transceiver A gets an estimated multipath CSI, $\mathbf{h}(t)$, for the channel between A and B, the corresponding TR signature is obtained as $\mathbf{g}(t) = \mathbf{h}^*(-t)$. As the transceiver A transmits back $\mathbf{g}(t)$ over the air, a spatial-temporal resonance is produced at transceiver B. The TR spatial-temporal resonance is generated by fully collecting the energy of the multipath channel and concentrating into a particular location. In physics, the spatial-temporal resonance is the result of a resonance of electromagnetic (EM) field in response to the environment, which can be used for capturing the difference in the multipath CSI.

TR was originally investigated in the phase compensation over telephone line [4] and was later extended to the acoustics [5] and the EM field [6]. The ability of TR technique in secured communication has been widely studied [3, 7, 8]. Additionally, a novel TR-based indoor localization approach was first proposed in [9], by mapping the physical location to the unique location-specific spatial-temporal resonance. Zhung-Han *et al.* built a prototype and implemented the system under

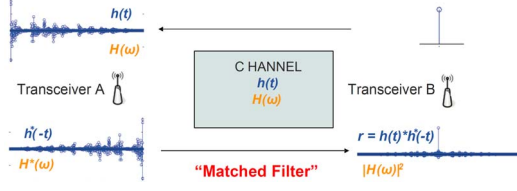


Fig. 1: TR-based wireless transmission.

a 125-MHz bandwidth, achieving a centimeter accuracy even with a single AP working in non-line-of-sight (NLOS) environments. Recently, in [10], a TR indoor locationing system on a WiFi platform was proposed and built, which utilizes the location-specific fingerprints generated by concatenating the CSI with a total equivalent bandwidth of 1 GHz. The accuracy can achieve 5 cm in NLOS locationing.

In the recent past, a number of attempts have been made to detect and recognize indoor human activities through wireless indoor sensing. Systems have been built to detect indoor human motions based on the variations of CSI [11–13]. Tracking and recording vital signals using wireless signal has been widely studied [14–16], as well as the recognition of gestures and small hand motions [17–19]. Recently, by sending a specially designed frequency modulated carrier wave (FMCW) which sweeps over different carrier frequencies in a total of 1 GHz band, Katabi *et al.* proposed a new radar-based system to keep track of the different time-of-flights (ToF) of the reflected signals [20, 21].

In this work, we propose a TR human identification system, which is the first to identify individuals through the walls, based on the human radio biometrics with WiFi signals. The system consists of two main algorithmic parts: the refinement of human radio biometrics and the TR-based identification. The system prototype consists of one 3-antenna transmitter (TX) and one 3-antenna receiver (RX), working on commodity WiFi chips. Moreover, the system is operated at carrier frequency 5.845 GHz with 40 MHz bandwidth. To the best of our knowledge, the proposed system is the first that utilizes commodity WiFi signals for human identification. The details of the proposed human identification system is discussed in Section 2. The performance of the proposed identification system is evaluated in Section 3. Our work demonstrates the potential of using commercial WiFi signals to capture human radio biometrics for individual identifications.

2. SYSTEM MODEL

Due to the multipath phenomenon, by sounding the WiFi CSI, the raw radio biometrics can be obtained, along with other channel information. The unique human radio biometrics are sufficient for the proposed system to differentiate between in-

dividuals through the wall.

Mathematically, with the presence of human body the indoor CSI (a.k.a. Channel frequency response, CFR) in the m^{th} link can be modeled as the sum of the common CSI component and the human affected component:

$$\mathbf{h}_i^{(m)} = \mathbf{h}_0^{(m)} + \delta\mathbf{h}_i^{(m)} + \mathbf{n}^{(m)}, \quad i = 1, 2, \dots, N, \quad (1)$$

where N is the number of individuals to be identified. The multipath profile $\mathbf{h}_i^{(m)}$ is a collection of all the reflected, scattered and direct paths of transmission in the environment. $\mathbf{h}_i^{(m)}$ is a $L \times 1$ complex-valued vector, which denotes the CSI when the i^{th} individual is inside. L is the number of subcarriers, i.e., the length of the CSI. $\mathbf{h}_0^{(m)}$, defined as the static CSI component, represents the propagation paths generated from the static environment in the absence of human and $\mathbf{n}^{(m)}$ represents the noise in estimating the CSI. $\delta\mathbf{h}_i^{(m)}$ is the raw human radio biometric information of the i^{th} individual embedding in the CSI of the m^{th} link, i.e., the paths in the wireless propagation introduced by the i^{th} individual.

At the receiver side, after each channel state sounding, we can collect a $L \times M$ raw CSI matrix for each individual as

$$\mathbf{H}_i = [\mathbf{h}_i^{(1)}, \mathbf{h}_i^{(2)}, \dots, \mathbf{h}_i^{(M)}], \quad \forall i, \quad (2)$$

and the corresponding human radio biometric information matrix is as

$$\delta\mathbf{H}_i = [\delta\mathbf{h}_i^{(1)}, \delta\mathbf{h}_i^{(2)}, \dots, \delta\mathbf{h}_i^{(M)}], \quad \forall i, \quad (3)$$

where M is the number of links between the transmitter and the receiver. The procedure for collecting the radio biometric information is called *radio shot*.

2.1. Time-Reversal Spatial-Temporal Resonance

As discussed in Section 1, the spatial-temporal resonance captures even minor changes in the multipath profiles, and it can be utilized to characterize the similarity between two vectors of multipath CSI. The strength of TR spatial-temporal resonance in frequency domain is defined as follows.

Definition: The strength of TR spatial-temporal resonance $\mathcal{TR}(\mathbf{h}_1, \mathbf{h}_2)$ in frequency domain between two CFRs \mathbf{h}_1 and \mathbf{h}_2 is defined as

$$\mathcal{TR}(\mathbf{h}_1, \mathbf{h}_2) = \frac{\max_{\phi} \left| \sum_k h_1[k] g_2[k] e^{jk\phi} \right|^2}{\left(\sum_{l=0}^{L-1} |h_1[l]|^2 \right) \left(\sum_{l=0}^{L-1} |h_2[l]|^2 \right)}. \quad (4)$$

Here, L is the length of CFR and \mathbf{g}_2 is the TR signature of \mathbf{h}_2 obtained as, $g_2[k] = h_2^*[k]$, $k = 0, 1, \dots, L-1$. The higher the value of $\mathcal{TR}(\mathbf{h}_1, \mathbf{h}_2)$ is, the more similar \mathbf{h}_1 and \mathbf{h}_2 are.

For two CSI measurement matrices \mathbf{H}_i and \mathbf{H}_j in a MIMO transmission, the spatial-temporal resonance strength between \mathbf{H}_i and \mathbf{H}_j is defined as the average on the spatial-temporal resonance strengths of all links, $\mathcal{TR}(\mathbf{H}_i, \mathbf{H}_j) = \frac{1}{M} \sum_{m=1}^M \mathcal{TR}(\mathbf{h}_i^{(m)}, \mathbf{h}_j^{(m)})$.

2.2. Radio biometrics Refinement Algorithm

However, without a refinement for the radio biometric information, the common feature which is of high energy in the CSI dominates in the spatial-temporal resonance strength, and thus the embedded human radio biometric information $\delta\mathbf{H}$ is small compared with other CSI components in measurement \mathbf{H} . The resulting spatial-temporal resonance strength $\mathcal{TR}(\mathbf{H}, \mathbf{H}_i)$ may become quite similar among different individuals and thus degrade system's ability of human identification. In this work, we propose postprocessing algorithms to extract the useful human radio biometric information from the CSI.

Considering the phase errors, each CSI sample $\mathbf{h}^{(m)}$ can be mathematically modeled as:

$$h^{(m)}[k] = \left| h^{(m)}[k] \right| \exp \left\{ -j(k\phi_{linear} + \phi_{ini}) \right\}, \quad (5)$$

$$k = 0, 1, \dots, L-1,$$

where ϕ_{linear} denotes the slope of the linear phase offset. ϕ_{ini} is the initial phase offset, and both of them are different among different CSI samples.

To address the phase misalignment among the CSI measurements, for each identification task, we align all the other CSI samples based on the reference, randomly picked in the training database. To begin with, we find the linear phase difference $\delta\phi_{linear}$ between the reference and each CSI sample. For each link, with any given CSI sample \mathbf{h}_2 and the reference \mathbf{h}_1 , we can have

$$\delta\phi_{linear} = \underset{\phi}{\operatorname{argmax}} \left| \sum_k h_1[k] h_2^*[k] \exp \left\{ jk\phi \right\} \right|. \quad (6)$$

After obtaining the difference $\delta\phi_{linear}$, the linear phase offset on \mathbf{h}_2 is cleaned by

$$\hat{h}_2[k] = h_2[k] \exp \left\{ -jk\delta\phi_{linear} \right\}, \quad k = 0, 1, \dots, L-1. \quad (7)$$

Once upon all the linear phase offsets have been compensated against the reference, the next step is to clean the initial phase offset in the CSI. The initial phase is viewed as the phase on the first subcarrier for each CSI sample $\angle\hat{h}[0]$, and can be compensated as $\mathbf{h}_{align} = \hat{\mathbf{h}} \exp \left\{ -j\angle\hat{h}[0] \right\}$.

In the following discussion, both the background and the refined human biometrics information are extracted from the aligned CSI measurements \mathbf{h}_{align} . To simplify the notation, we will use \mathbf{h} instead of \mathbf{h}_{align} to denote the aligned CSI in the rest of the paper.

As in the proposed CSI model in (1), $\mathbf{h}_i^{(m)}$ can be further decomposed as following:

$$\mathbf{h}_i^{(m)} = \mathbf{h}_0^{(m)} + \delta\mathbf{h}_{i,c}^{(m)} + \delta\mathbf{h}_{i,c}^{(m)} + \hat{\mathbf{n}}^{(m)}, \quad \forall i, m, \quad (8)$$

where $\mathbf{h}_i^{(m)}$ and $\hat{\mathbf{n}}^{(m)}$ denote the CSI and the noise after phase alignment. The radio biometric is further decomposed

as $\delta\mathbf{h}_i^{(m)} = \delta\mathbf{h}_{i,c}^{(m)} + \delta\mathbf{h}_{i,c}^{(m)} \cdot \delta\mathbf{h}_{i,c}^{(m)}$ denotes the common radio biometric information, which is possessed and determined by all the participants in the identification system, and $\delta\mathbf{h}_{i,c}^{(m)}$ is the distinct radio biometric information for identification.

The background CSI components for several CSI measurements of N individuals can be estimated by taking the average over the aligned CSI as:

$$\mathbf{h}_{bg}^{(m)} = \frac{1}{N} \sum_{i=1}^N \frac{\mathbf{h}_i^{(m)}}{\left\| \mathbf{h}_i^{(m)} \right\|^2}. \quad (9)$$

Then the distinct human radio biometrics for each individual can be extracted through subtracting a scaled version of the background in (9) from the original CSI. $\tilde{\mathbf{h}}_i^{(m)} = \mathbf{h}_i^{(m)} - \alpha\mathbf{h}_{bg}^{(m)}$, where α is the background subtraction factor, $0 \leq \alpha \leq 1$. When α approaches to 1, the remaining CSI is noise-like.

2.3. Identification Methodology

After taking the radio shot, by means of the TR technique, the high-dimension complex-valued human radio biometrics embedded in the CSI measurements are mapped into the space of the spatial-temporal resonance strength, and the feature dimension is reduced from $L \times M$ to 1. The human identification problem can be implemented as a simple multi-class classification problem as following.

For any CSI measurement \mathbf{H} , given a training database consisting of the CSI of each individual \mathbf{H}_i , $\forall i$, the predicted individual identity (ID) is obtained based on the TR spatial-temporal resonance strength after biometric refinement as:

$$\hat{i} = \begin{cases} \underset{i}{\operatorname{argmax}} \mathcal{TR}(\tilde{\mathbf{H}}, \tilde{\mathbf{H}}_i), & \text{if } \max_i \mathcal{TR}(\tilde{\mathbf{H}}, \tilde{\mathbf{H}}_i) \geq \mu, \\ 0, & \text{otherwise,} \end{cases} \quad (10)$$

where μ is a predefined threshold for triggering the identification, and $\hat{i} = 0$ denotes an unidentified individual. $\tilde{\mathbf{H}}$ is the refined radio biometric information matrix from measurement \mathbf{H}_i and can be viewed as an approximation of the distinctive component in the human radio biometric information matrix $\delta\mathbf{H}$ defined in (3).

3. PERFORMANCE EVALUATION

In this section, the performance of human identification is evaluated using the prototype. The evaluation experiments are conducted in the office at the 10th floor of a commercial office building with a total of 16 floors. The floorplan of the experiment office is shown in Figure 2. Surrounding the experiment office, there are 4 elevators and multiple occupied offices. All the experiments are conducted during the normal working hours in weekdays, so that outside the experiment

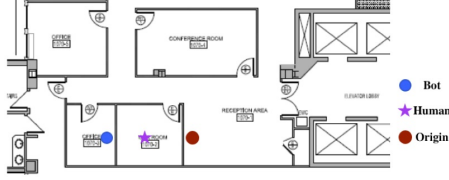


Fig. 2: Experiment settings: configurations.

		Testing Data					
		Empty room	Human #1	Human #2	Human #3	Human #4	Human #5
Training Data	Empty room	1	0	0	0	0.4944	0.9613
	Human #1	0	1	0	0.5754	0.4138	0
	Human #2	0	0	1	1	0.9974	1
	Human #3	0	0.3159	1	1	0.1912	0.8869
	Human #4	0.8722	0.4951	0.9917	0.5672	1	1
	Human #5	0.9781	0	1	0.9999	1	1

(a) No background subtraction.

(b) After background subtraction with $\alpha = 0.5$.

Table 1: Performance matrices for individual identification with and without background subtraction.

office there are many activities, such as human walking and elevator running, happening in the course of experiments.

In Figure 2 the experiment configurations of the transmitter, receiver and individuals are demonstrated. The distance between the transmitter and the receiver is about 3 meters, with two walls in-between. To take the radio shot, each individual stands in the room on the point marked by the purple star and the door of this room is closed. Furthermore, in the experiments, we build the training database with 50 CSI measurements for each class, while the size of the testing database for identification is 500 CSI samples per class.

3.1. Impact of Background Subtraction

To begin with, we first quantitatively study the impact of the proposed postprocessing algorithms for background subtraction and biometrics refinement by conducting experiments to differentiating between 5 individuals. In Table 1, each element in the tables is the probability of the case when the resonating strength between the training class and the testing class is higher than the threshold μ as defined in (10). For the sake of a fair comparison, we set the detection threshold $\mu = 0.9$ for both experiments.

Without background subtraction, the correct identification rate can reach 100% indicated by the diagonal elements. However, the false alarm rate, i.e., the probability of being identified as other training classes when the class of testing samples is not in the database, can be as high as 99.99%. After background subtraction, when using the refined radio biometrics for identification, the highest false alarm rate is 0.24% while the lowest detection rate is 96.35% as shown in Table 1b. Through the refinement, the TR spatial-temporal resonance between different classes is suppressed a lot while

maintaining a high strength within the same class.

3.2. Human Identification

In this part, the performance is evaluated in a large data set of 11 individuals, with background subtraction applied. The corresponding ROC curve is plotted in Figure 3, obtained by adjusting μ in (10). With a threshold μ being 0.91, the average detection rate is 98.78% and the average false alarm rate is 9.75%. This is because, when two individuals have similar body contour, the possibility of misclassifying between them increases. However, since not only the contour but also the permittivity and conductivity of body tissue, which is more unique for different individuals, will affect the WiFi signal propagation that encounters the human body, the accuracy of human recognition is still high.

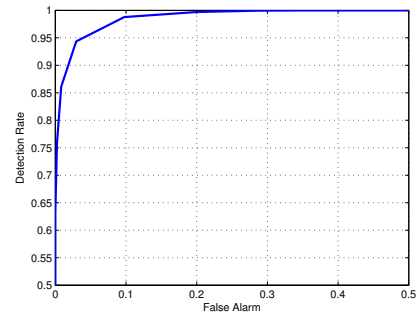


Fig. 3: ROC curve of identifying 11 individuals.

4. CONCLUSIONS

We propose a TR human identification system, where individuals are distinguished from and identified by the human radio biometrics extracted from the WiFi CSI through the TR technique. Furthermore, the existence of the human radio biometrics, which can be found embedding in the indoor WiFi signal propagation, is shown and verified in this work. By leveraging the TR technique to extract radio biometrics, a low-complexity human identification system can be widely implemented without restrictions on the device deployment thanks to the ubiquitousness of WiFi.

5. REFERENCES

- [1] Anil Jain, Arun A Ross, and Karthik Nandakumar, *Introduction to biometrics*, Springer Science & Business Media, 2011.
- [2] Petr Beckmann and Andre Spizzichino, "The scattering of electromagnetic waves from rough surfaces," *Norwood, MA, Artech House, Inc., 1987, 511 p.*, 1987.

- [3] Beibei Wang, Yongle Wu, Feng Han, Yu-Han Yang, and K. J. R. Liu, "Green wireless communications: A time-reversal paradigm," *IEEE Journal on Selected Areas in Communications*, vol. 29, no. 8, pp. 1698–1710, 2011.
- [4] B. Bogert, "Demonstration of delay distortion correction by time-reversal techniques," *IRE Transactions on Communications Systems*, vol. 5, no. 3, pp. 2–7, December 1957.
- [5] Mathias Fink, Claire Prada, Francois Wu, and Didier Cassereau, "Self focusing in inhomogeneous media with time reversal acoustic mirrors," *IEEE Ultrasonics Symposium Proceedings*, pp. 681–686, 1989.
- [6] Geoffroy Lerosey, J De Rosny, A Tourin, A Derode, G Montaldo, and M Fink, "Time reversal of electromagnetic waves," *Physical review letters*, vol. 92, no. 19, pp. 193904, 2004.
- [7] Yan Chen, Feng Han, Yu-Han Yang, Hang Ma, Yi Han, Chunxiao Jiang, Hung-Quoc Lai, David Claffey, Zoltan Safar, and K. J. R. Liu, "Time-reversal wireless paradigm for green internet of things: An overview," *IEEE Internet of Things Journal*, vol. 1, no. 1, pp. 81–98, 2014.
- [8] Qinyi Xu, Yan Chen, and K. J. R. Liu, "Combating strong-weak focusing effect in time-reversal uplinks," *IEEE Transactions on Wireless Communications*, vol. 15, no. 1, pp. 568–580, Jan 2016.
- [9] Zhong-Han Wu, Yi Han, Yan Chen, and K. J. R. Liu, "A time-reversal paradigm for indoor positioning system," *IEEE Transactions on Vehicular Technology*, vol. 64, no. 4, pp. 1331–1339, April 2015.
- [10] Chen Chen, Yan Chen, K. J. Ray Liu, Yi Han, and Hung-Quoc Lai, "High-accuracy indoor localization: A wifi-based approach," *the 41st IEEE International Conference on Acoustics, Speech and Signal Processing (ICASSP)*, 2016.
- [11] Jiang Xiao, Kaishun Wu, Youwen Yi, Lu Wang, and L.M. Ni, "Fimd: Fine-grained device-free motion detection," in *Proceedings of the 18th International Conference on Parallel and Distributed Systems (ICPADS)*, Dec 2012, pp. 229–235.
- [12] Wei Wang, Alex X Liu, Muhammad Shahzad, Kang Ling, and Sanglu Lu, "Understanding and modeling of WiFi signal based human activity recognition," in *Proceedings of the 21st Annual International Conference on Mobile Computing and Networking*. ACM, 2015, pp. 65–76.
- [13] Wei Xi, Jizhong Zhao, Xiang-Yang Li, Kun Zhao, Shaojie Tang, Xue Liu, and Zhiping Jiang, "Electronic frog eye: Counting crowd using WiFi," in *Proceedings of the International Conference on Computer Communications (INFOCOM)*, April 2014, pp. 361–369.
- [14] Jian Liu, Yan Wang, Yingying Chen, Jie Yang, Xu Chen, and Jerry Cheng, "Tracking vital signs during sleep leveraging off-the-shelf WiFi," in *Proceedings of the 16th ACM International Symposium on Mobile Ad Hoc Networking and Computing*, New York, NY, USA, 2015, MobiHoc '15, pp. 267–276, ACM.
- [15] Fadel Adib, Hongzi Mao, Zachary Kabelac, Dina Katabi, and Robert C. Miller, "Smart homes that monitor breathing and heart rate," in *Proceedings of the 33rd Annual ACM Conference on Human Factors in Computing Systems*, New York, NY, USA, 2015, CHI '15, pp. 837–846, ACM.
- [16] R. Ravichandran, E. Saba, K. Y. Chen, M. Goel, S. Gupta, and S. N. Patel, "Wibreathe: Estimating respiration rate using wireless signals in natural settings in the home," in *Proceedings of the International Conference on the Pervasive Computing and Communications (PerCom)*, March 2015, pp. 131–139.
- [17] Qifan Pu, Sidhant Gupta, Shyamnath Gollakota, and Shwetak Patel, "Whole-home gesture recognition using wireless signals," in *Proceedings of the 19th Annual International Conference on Mobile computing & networking*. ACM, 2013, pp. 27–38.
- [18] Li Sun, Souvik Sen, Dimitrios Koutsonikolas, and Kyu-Han Kim, "Withdraw: Enabling hands-free drawing in the air on commodity WiFi devices," in *Proceedings of the 21st Annual International Conference on Mobile Computing and Networking*. ACM, 2015, pp. 77–89.
- [19] Kamran Ali, Alex Xiao Liu, Wei Wang, and Muhammad Shahzad, "Keystroke recognition using WiFi signals," in *Proceedings of the 21st Annual International Conference on Mobile Computing and Networking*. ACM, 2015, pp. 90–102.
- [20] Fadel Adib, Zachary Kabelac, and Dina Katabi, "Multi-person localization via RF body reflections," in *Proceedings of the 12th USENIX Symposium on Networked Systems Design and Implementation (NSDI 15)*, Oakland, CA, May 2015, pp. 279–292, USENIX Association.
- [21] Fadel Adib, Chen-Yu Hsu, Hongzi Mao, Dina Katabi, and Frédo Durand, "Capturing the human figure through a wall," *ACM Transactions on Graphics*, vol. 34, no. 6, pp. 219:1–219:13, Oct. 2015.